Making Flanged Nanobearings with Carbon Nanotubes

Prathamesh Mahesh Shenai and Yang Zhao*
School of Material Science and Engineering, Nanyang Technological University, Singapore 639798

Introduction

Following the pioneering experimental demonstration by Cumings et al. of multiwalled carbon nanotubes (MWNTs) serving as oscillators with unparalleled small frictional resistance [1], erupted entirely new nanomechanics based on carbon nanotubes [2-6]. Being the simplest model, double walled carbon nanotubes (DWNTs) have been studied extensively using molecular dynamics simulations as linear or rotational bearings. Atomically, smooth contacting surfaces between the nested shells of a DWNT lead to the possibility of wearless nanomachines. Study of rotational nanobearings with a rotating inner tube by Zhang et al. [2] revealed a velocity threshold below which there exists a wearless operating regime. Frictional drag in nanobearings is found to be proportional to the area of contact and significantly dependent upon rotational velocity as well as the operating temperature [6]. To broaden the smooth working domain of a nanobearing, we present, in this paper, a new approach to design a flanged bearing by manipulating the DWNT structure.

Design and Methodology

We propose a new design of nanobearing based on DWNTs. The inner tube, called as the shaft, is designed by joining two 3 nm long (8,0) SWNTs to either ends of a 4 nm long (4,4) armchair SWNT. Since the diameter of (8,0) nanotube is larger than that of (4,4), a shoulder is formed at their junction. Due to the difference in the diameter at the junction, connection between two nanotubes is facilitated by alternate pentagons and heptagons along the circumference such that the co-linearity of the tubes can be preserved while still obeying Euler's rule. The outer tube, also called as the sleeve, is designed in exactly the same way by connecting two (18,0) SWNTs to the ends of a (9,9) nanotube. The composite structure formed assumes the form of a flanged nanobearing as shown in Fig.1. The overall length of the flanged bearing is 10nm. Hence the flanged bearing structure encompasses two bearing systems, (4,4)/(9,9) –as the central part and (8,0)/(18,0) –as the lateral part. Due to the flanges on either side of the central part, an intrinsic barrier against axial translational motion of the inner tube is set up. During the operation of the nanobearing, the dissipation of its rotational energy into axial translational energy is inhibited, resulting in improved bearing performance.

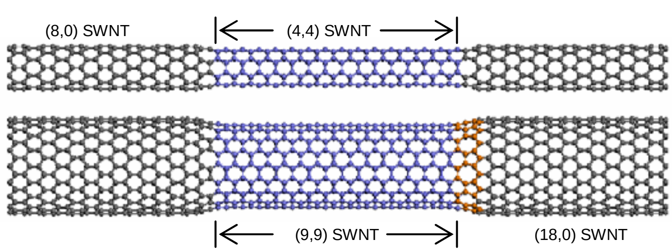

Fig.1 Design scheme for the flanged nano bearing with the inner tube at top and outer tube at bottom.. The connection achieved by alternate heptagons-pentagons is illustrated in the orange highlighted portion.

We carry out classical molecular dynamics simulations of the flanged nanobearing using a microcanonical ensemble. In all our simulations, the shaft is the rotator of the bearing and a certain initial angular velocity is ascribed to every atom of the shaft. Three atoms at each end of the sleeve have been pinned down at their initial positions. Both the initial geometry optimization and the ensuing molecular dynamics calculations are performed using the Dreiding forcefield utilizing the Lennard-Jones potential (LJ 12-6 form) for van der Waals interactions [3]. A step size of 1fs is used. In order to examine high-temperature effects, first equilibration of the nanobearing is performed at 300K for 300ps. Following this, an initial angular velocity is assigned to the inner tube and the dynamics is studied in the microcanonical ensemble. For the purpose of comparison with the flanged bearing, we use a uniform (4,4)/(9,9) DWNT bearing composed of (4,4) nanotube as the shaft and (9,9) tube as the sleeve, both of an equal length of nearly 10nm.

Results and Discussion

Bearing characteristics have been studied upon subjecting the shaft to a ranged of initial angular velocities ω. For a simulation time of 1 ns, Fig. 2 displays the angular velocity dampening with time for various initial angular velocities (ω= 1, 3, 5, 8 and 10 rad/ps) with no pre-simulation heating. The simple (4,4)/(9,9) bearing enters into a strongly dissipative regime except at low ω of 1 rad/ps; whereas the flanged bearing maintains its angular velocity without any appreciable dissipation until 5 rad/ps suggesting nearly frictionless behavior. Even at an extremely high ω of 10 rad/ps, the flanged bearing shows considerable energy dissipation with only 14% reduction in its initial angular velocity as compared to 98.5% slowdown of the (4,4)/(9,9) bearing. Results extend in similar ways, when the bearing is tested at an elevated pre-simulation temperature of 300K. In the high temperature operation, the shaft rotations are damped faster for both bearings. However, the flanged bearing maintains its angular velocity appreciably for initial velocities at or below

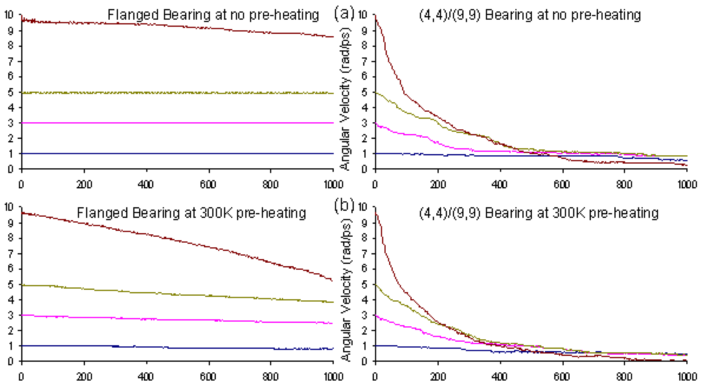

Fig.2 Angular velocity dissipation for the flanged bearing and the (4,4)/(9,9) bearing with initial angular velocity as 1 rad/ps, 3 rad/ps, 5rad/ps and 10 rad/ps. Top and bottom panels show the results with 0K (i.e., no heating) and 300K pre-simulation temperature, respectively.

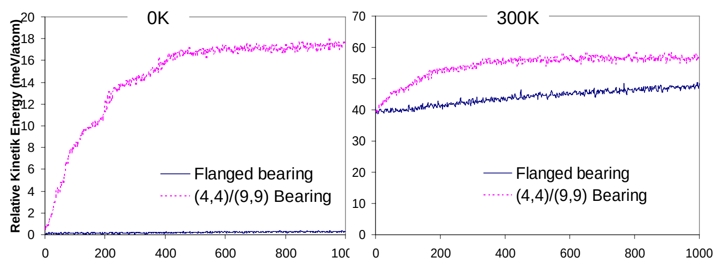

Fig. 3 Comparison of relative kinetic energy (meV/atom) for flanged bearing and (4,4)/(9,9) bearing at ω=3 rad/ps and no pre-simulation heating (left) and with pre-simulation heating to 300K (right)

5 rad/ps. High speed as well as high temperature stability is thus evident of the amelioration brought about by the structural manipulation in creating the flanged bearing.

As the inner tube starts to rotate, the rotational kinetic energy can be channelled into various mechanical modes while its significant fraction is expended to excite the phonon modes in the two tubes. The amount of this energy is in direct correlation with the energy dissipation due to friction. Relative kinetic energy (RKE) serves as a direct measurement of disorderly phonon energy and is calculated after subtracting group translational and rotational kinetic energy components from the total kinetic energy of both the nanotubes [4]. As displayed in Fig. 2, the RKE is at least an order of magnitude lower for the flanged bearing in comparison with the (4,4)/(9,9) bearing when ω = 3 rad/ps. It is negligibly low even for moderately high ω in case of the flanged bearing without pre-simulation heating showing extremely small amount of energy acquired by phonons. At 300K, the RKE, although comparable, is still smaller for flanged bearing than for the plain bearing.

Due to the intrinsic barrier against intertube axial motion, the flanged bearing shows much less transfer from the rotational kinetic energy to its translational counterpart. The inner tube of the flanged bearing is thus axially confined in a steeper potential well against axial sliding than the simple bearing as is clearly exhibited in Fig.4. The shoulders formed near an axial displacement of 3.6 nm are the result of our flanged structural design.As shown in the inset

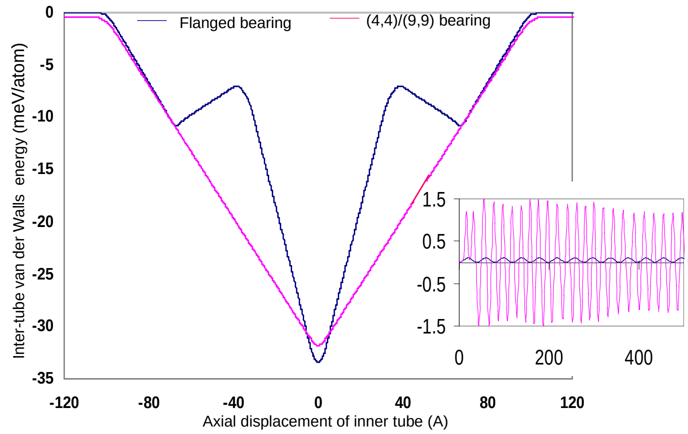

Fig.4 Van der Waals potential energy variation versus axial sliding for the flanged bearing and (4,4)/(9,9) bearing. Inset shows axial oscillation of inner tube for both types of bearings when ω=3rad/ps

of Fig. 4, in comparison, the uniform DWNT bearing shows pronounced axial oscillation whereas the flanged one oscillates in a narrow range. At elevated temperatures, the atoms of the inner tube can acquire enough energy to overcome sliding barrier in the case of the simple bearing. However, due to the steeper potential well in which the inner tube of flanged bearing resides, even at high pre-simulation temperature restriction on axial motion is preserved. Further, the (8,0)/(18,0) end segments have the intertube distance of about 0.39 nm which is higher than the equilibrium distance of 0.34 nm between adjacent tubes in an MWNT. As a result, the Van der Waals interaction between the two tubes is small and results in extremely shallow corrugation against rotation permitting smoother rotation. On the other hand, the separation is not large enough to affect the symmetry of the DWNT bearing thereby providing it axial stability. Recent experimental techniques for tuning CNT diameter by temperature variation may lead to feasibility of flanged structures [5].

Conclusion

A new design of DWNT-based nanobearings is introduced. The features of the flanged nanobearing have been shown to significantly better the performance via inhibition of large amplitude axial motion of the rotator thereby yielding low energy dissipation and wider operating regime.

References

* yzhao@ntu.edu.sg

1. Cumings, J. and Zettl, A. *Science* **289,** 602-604 (2000).
2. Zhang S., Liu W. K. and Ruoff, R. S. *Nano Lett.* **4** , 293-297 (2004).
3. Mayo, S. L., Olafson, B. D. and Goddard, W. A. *J. Phys. Chem.* **94**, 8897-8909 (1990).
4. Zhao, Y., Ma, C.C., Chen G.H. and Jiang, Q. Phys. Rev. Lett. **91,** 175504 (2003).
5. Yao, Y. , Li, Q., Zhang, J., Liu, R. ., Jiao, L., Zhu, Y.T. and Liu, Z. *Nat. Mat*. **6,** 293-296 (2007).
6. Zhu, B.E., Pan. Z. Y., Wang, Y.X., and Xiao, Y. *Nanotechnology* **19**, 495708 (2008).